Received: 16 April 2022 | Revised: 18 July 2022 | Accepted: 4 August 2022

DOI: 10.1002/hbm.26058

RESEARCH ARTICLE

WILEY

Alterations of voxel-wise spontaneous activity and corresponding brain functional networks in multiple system atrophy patients with mild cognitive impairment

Yingmei Li[1] | Hu Liu[1] | Hongmei Yu[2] | Huaguang Yang[3] | Miaoran Guo[1] | Chenghao Cao[4] | Huize Pang[1] | Yu Liu[1] | Kaiqiang Cao[1] | Guoguang Fan[1]

[1]Department of Radiology, The First Hospital, China Medical University, Shenyang, Liaoning, China

[2]Department of Neurology, The First Hospital, China Medical University, Shenyang, Liaoning, China

[3]Department of Radiology, Renmin Hospital, Wuhan University, Wuhan, Hubei, China

[4]Department of Radiology, West China Hospital, Sichuan University, Chengdu, Sichuan, China

Correspondence
Guoguang Fan, Department of Radiology, The First Hospital, China Medical University, Shenyang, Liaoning, China.
Email: fanguog@sina.com

Funding information
National Natural Science Foundation of China, Grant/Award Number: 82071909

Abstract

Emerging evidence has indicated that cognitive impairment is an underrecognized feature of multiple system atrophy (MSA). Mild cognitive impairment (MCI) is related to a high risk of dementia. However, the mechanism underlying MCI in MSA remains controversial. In this study, we conducted the amplitude of low-frequency fluctuation (ALFF) and seed-based functional connectivity (FC) analyses to detect the characteristics of local neural activity and corresponding network alterations in MSA patients with MCI (MSA-MCI). We enrolled 80 probable MSA patients classified as cognitively normal (MSA-NC, $n = 36$) and MSA-MCI ($n = 44$) and 40 healthy controls. Compared with MSA-NC, MSA-MCI exhibited decreased ALFF in the right dorsal lateral prefrontal cortex (RDLPFC) and increased ALFF in the right cerebellar lobule IX and lobule IV–V. In the secondary FC analyses, decreased FC in the left inferior parietal lobe (IPL) was observed when we set the RDLPFC as the seed region. Decreased FC in the bilateral cuneus, left precuneus, and left IPL and increased FC in the right middle temporal gyrus were shown when we set the right cerebellar lobule IX as the seed region. Furthermore, FC of DLPFC-IPL and cerebello-cerebral circuit, as well as ALFF alterations, were significantly correlated with Montreal Cognitive Assessment scores in MSA patients. We also employed whole-brain voxel-based morphometry analysis, but no gray matter atrophy was detected between the patient subgroups. Our findings indicate that altered spontaneous activity in the DLPFC and the cerebellum and disrupted DLPFC-IPL, cerebello-cerebral networks are possible biomarkers of early cognitive decline in MSA patients.

KEYWORDS
amplitude of low-frequency fluctuation, functional connectivity, mild cognitive impairment, multiple system atrophy, resting-state network

Yingmei Li and Hu Liu shared the first authorship.

1 | INTRODUCTION

Multiple system atrophy (MSA) is a sporadic, adult-onset, progressive neurodegenerative disease characterized by various combinations of autonomic failure, parkinsonism, cerebellar ataxia, and pyramidal signs (Gilman et al., 2008; Quinn, 1989, 2020). Cognitive dysfunction is traditionally believed to be rare in MSA (Wenning et al., 1997), and dementia is even considered a nonsupporting feature in the current consensus diagnostic criteria for MSA (Gilman et al., 2008). However, accumulating evidence has indicated that cognitive decline is an integral part of MSA (Stankovic et al., 2014), and the prevalence rates of cognitive impairment (CI) in MSA range from 22% to 37% in autopsy-confirmed MSA patients (Cykowski et al., 2015; Homma et al., 2016; Koga et al., 2015; Wenning et al., 1997). Frontal executive function is most commonly affected in MSA patients, whereas attention, memory, and visuospatial domains are only sometimes impaired (Koga et al., 2017; Stankovic et al., 2014). The spectrum of cognitive function in MSA spans from normal cognition through mild cognitive impairment (MCI) to MSA patients with dementia (Stankovic et al., 2014). MCI, in which the functional impact of CI is not severe enough to impair daily life, is the most common cognitive syndrome in MSA (Fiorenzato, Antonini, et al., 2017). Recognizing MCI in MSA is critical in clinical settings, as affected individuals are likely to progress toward dementia (Sambati et al., 2020; Stankovic et al., 2014). MCI in MSA patients has detrimental implications for life satisfaction, caregiver burden, and health-related costs (Stankovic et al., 2014; Zhang et al., 2019).

To date, the underlying neuropathological mechanism of MSA-related MCI remains unclear. A battery of morphological MRI studies indicated that atrophy in MSA patients occurs in widespread cortical regions as well as subcortical regions, including the striatum, mesencephalon, thalamus, and cerebellum (Stankovic et al., 2014). In surface-based shape analysis (Lee et al., 2016), MSA patients with prominent cerebellar ataxia (MSA-C) showed cognition-related atrophic changes in the frontotemporoparietal cortices and the bilateral thalamus, the left cerebellum, and the left pericalcarine gyrus. Similarly, in MSA patients with prominent parkinsonism (MSA-P), voxel-based morphometry (VBM) and thickness analysis were combined, and the cognitive dysfunction was shown to be significantly correlated with thinning in the neocortex, cerebellum, and striatum (Kim et al., 2015), supporting the concept of subcortical CI. Conversely, Caso et al. (2020) found that, although cortical thinning and subcortical atrophy coexist in MSA-P patients, CI is related to cortical thinning in temporal regions, indicating primary cortical involvement (Cao et al., 2021; Chang et al., 2009). However, whether CI in MSA results from primary cortical damage or subcortical degeneration with secondary cortical deafferentation remains controversial. Resting-state functional magnetic resonance imaging (rs-fMRI) has become an increasingly popular tool for investigating the pathogenesis of neurological and mental diseases (Biswal, 2012). Limited research has employed rs-fMRI to characterize cognition-related network alterations in MSA patients. In these studies, Yang, Wang, Luo, Lv, Liu, and Fan (2019a) found functional connectivity (FC) of the right dentate nucleus and right cerebellum was correlated with cognitive behaviors in MSA patients. In further research, Yang et al. (2020) combined degree centrality (DC) and secondary FC analysis, and detected disruptions of the dorsolateral prefrontal cortex (DLPFC)-default mode network (DMN) and DLPFC-insula network in MSA patients with CI (MSA-CI). Kawabata et al. (2019) used independent component analysis (ICA) to define the seeds and found altered FC of the cerebello-prefrontal and cerebello-amygdala networks in MSA patients, which were correlated with cognitive function. However, the characteristics of local brain activity in MSA-CI were not well defined. The amplitude of low-frequency fluctuation (ALFF) is a reliable and stable metric in rs-fMRI (Zuo & Xing, 2014), examining regional brain activity at the voxel level (Zang et al., 2007). Previous studies have observed ALFF alterations in Parkinson's disease (PD), MCI with depression, and early Alzheimer's disease (He et al., 2007; Liu et al., 2019; Wang et al., 2020). However, ALFF analysis has not been employed in MSA-MCI.

Moreover, altered focal spontaneous activity may underlie correlation disruptions with other brain regions. Seed-based FC analysis measures the correlation coefficients of a pre-defined region with other brain regions (Friston, 2011). Existing seed-based FC analyses in MSA-CI chose the seed regions based on network metrics results (Kawabata et al., 2019; Yang et al., 2020) or prior literature (Yang, Wang, Luo, Lv, Liu, & Fan, 2019a). Corresponding network alterations based on regional neural activity changes have not been investigated. ALFF and FC analyses have been combined to better characterize brain function in several neurodegenerative and psychiatric disorders, including PD (Skidmore et al., 2013) with freezing of gait (Hu et al., 2020), CI-related disorders (Hu et al., 2020), major depressive disorder (Yan et al., 2022), and amnestic CI (Cai et al., 2017). In this study, we aimed to combine ALFF and FC analyses to characterize the regional brain activity alterations and corresponding network changes related to early cognitive decline in MSA-MCI. We also employed VBM analysis to see whether morphological changes were consistent with our functional findings, which could provide deeper insight into disease progression. We hypothesized that regional intrinsic activity alterations, as well as associated brain network dysfunction, may contribute to MCI in MSA patients.

2 | MATERIALS AND METHODS

2.1 | Participants

A total of 80 MSA patients (42 MSA-C patients and 38 MSA-P patients) were enrolled at the First Hospital of China Medical University. Furthermore, 40 healthy controls matched for gender, age, and education, with no history of neuropsychiatric disease, were also recruited. Patients were diagnosed as having probable MSA based on the second consensus clinical criteria (Gilman et al., 2008) by a movement disorder specialist. Patients who had a history of other neurological or psychiatric disorders were excluded. All patients were off antiparkinsonian medications for at least 12 h prior to the scan. All

subjects were right-handed. Participants with any neuroanatomical abnormalities detectable under conventional MRI were excluded. The study was approved by the Ethics Committee of the First Hospital of China Medical University, and written informed consent was obtained from each participant.

2.2 | Diagnostic criteria and clinical measurement

We systematically collected the demographic and clinical information of each participant, including age, gender, years of education, disease duration, and drug dose. For patients, the Hoehn and Yahr (H & Y) scale was used to measure disease stage, and the severity of motor disability was evaluated with the Unified Multi-System Atrophy Scale-Part II (UMSARS-II).

All participants underwent neuropsychological assessments including the Mini-Mental State Examination (MMSE), the Montreal Cognitive Assessment (MoCA), and the Hamilton Depression Scale (HAMD-24). We first excluded MSA patients with dementia (MSA-D). Since no diagnostic criteria for MSA-D were available, we referred to the diagnostic criteria of Parkinson's disease dementia (PDD) (a): MMSE score ≤25, (b) cognitive deficiency severe enough to affect daily life, and (c) more than one cognitive domain impaired (Dubois et al., 2007). Based on the Movement Disorder Society diagnostic criteria (Litvan et al., 2012), a diagnosis of MSA-MCI was defined as (a) gradual decline of cognitive function, (b) MoCA score ≤25 (MoCA score ≤24 for those with less than 12 years of education), and (c) CI not severe enough to affect daily life. Patients who did not fulfill the criteria of MSA-MCI were considered MSA-NC.

2.3 | Image acquisition

All participants underwent MRI scanning in a 3.0T MRI scanner (Magnetom Verio, Siemens, Erlangen, Germany) equipped with a 32-channel head coil at the First Hospital of China Medical University. A high-resolution three-dimension sagittal magnetization-prepared rapid acquisition gradient echo (MPRAGE) T1-weighted sequence was obtained with the following parameters: repetition time (TR) = 5000 ms, echo time (TE) = 2960 ms, flip angle (FA) = 12°, field of view (FOV) = 256 cm^2, dist. factor = 0.5, matrix size = 256 × 256, voxel size = 1.0 × 1.0 × 1.0 mm, slice number = 176, slice thickness = 1 mm. The resting-state functional images were acquired using a gradient echo planar imaging sequence with the following parameters: TR = 2500 ms, TE = 30 ms, flip angle = 90°, slice number = 43, slice thickness = 3.5 mm without a slice gap, FOV = 224 mm^2, matrix size = 64 × 64, and voxel size = 3.5 × 3.5 × 3.5 mm.

Each subject was instructed to rest with their eyes closed but be awake during the scan, thinking of nothing in particular. We routinely confirmed that they had remained awake and kept their minds blank in the process.

2.4 | Rs-fMRI data preprocessing

Resting-state fMRI data were preprocessed and further analyzed with the Data Processing & Analysis for (Resting-State) Brain Imaging (DPABI) toolbox (version 3.0, www.restfmri.net). The preprocessing steps were as follows: (a) discarding the first 10 time points of each participant to avoid magnetic saturation effects and for participants to adapt to the scanning noise; (b) slice timing; (c) head motion correction (subjects with more than 2.5 mm displacement in any of *x*, *y*, and *z* directions or 2.5° of angular rotation were removed); (d) co-registration, spatial normalization, and resampling to 3 × 3 × 3 mm resolution; (e) spatial smoothing with an isotropic Gaussian kernel at full width and half maximum (FWHM) of 6 mm; (f) removing the linear trend and regressing nuisance covariates, including the Friston-24 head motion parameters (Friston et al., 1996), global BOLD signals, and signals of white matter and cerebrospinal fluid (CSF).

2.5 | ALFF analysis

Fast Fourier transform was conducted to transform the whole-brain voxel-wise time series in the time domain into a frequency domain and gain the power spectrum. Temporal band-pass filtering (0.01–0.08 Hz) was performed to acquire ALFF maps. Then, we transformed the ALFF maps to the zALFF maps with *z*-score transformation for further analysis.

2.6 | FC analysis

Based on the ALFF results, we performed seed-based FC analysis. Brain regions showing ALFF alterations between MSA-MCI and MSA-NC, and further correlated with MoCA scores were selected as seed regions. We obtained three seed regions, including the right dorsal lateral prefrontal gyrus (RDLPFC), which peak Montreal Neurological Institute (MNI) coordinate is (42, 33, 15), the right cerebellar lobule IX (rCbe9), which peak MNI coordinate is (27, −45, −21), and the right cerebellar lobule IV–V (rCbe4-5), which peak MNI coordinate is (18, −48, −48). Each seed was set in a sphere with a radius of 3 mm around the center voxels. The reference time series of each seed was obtained by averaging the time series of all voxels in the seed region. The Pearson's correlation coefficients were computed between the time course of each seed region and the time courses of all other voxels in the brain. The correlation coefficients were ultimately converted into *z*-values by applying Fisher's *r*-to-*z* transformation to achieve normality. Seed-to-voxel FC maps were estimated for each subject.

2.7 | VBM analysis

We conducted a whole-brain VBM analysis to detect gray matter (GM) volume reduction among groups using the Computational Anatomy Toolbox (CAT12) in Statistical Parametric Mapping (SPM12)

software (Wellcome Department of Imaging Neuroscience, London, UK). T1 images were spatially registered to the MNI space and segmented into white matter (WM), GM, and CSF. Segmented images of the GM were modulated, and the modulated normalized GM maps were then smoothed using an 8-mm FWHM Gaussian kernel for further analysis. We also estimated the total intracranial volume (TIV) for each participant.

2.8 | Statistical analysis

Statistical analysis of demographic and clinical data was performed using SPSS 20.0 software (IBM Software Analytics, New York, NY). Non-normally distributed data, such as age, education level, MoCA, and MMSE scores, among the three groups were evaluated using the Kruskal–Wallis *H* test. The chi-square test was used to assess the gender distribution. Disease duration, UMSARS-II scores, and H–Y stage were compared between patient groups using the Mann–Whitney *U* test. The correlation between functional alterations and clinical data was analyzed using the Spearman rank correlation analysis. The statistical thresholds above were set at .05 (two-tailed).

Voxel-wise statistical analysis for imaging data was calculated in SPM12. We conducted a one-way ANOVA to explore ALFF differences among the MSA-MCI, MSA-NC, and HC groups, with age, gender, disease duration, education, and levodopa equivalent dose as covariates. Multiple comparisons were performed using the Gaussian random field (GRF) correction, and the cluster-level statistical threshold was set at $p < .05$, while the voxel-level threshold was set at $p < .001$. Post hoc analysis was then carried out to evaluate between-group differences within the mask with significant ANOVA differences sharing the same covariates and the multiple comparison correction methods with ANOVA (GRF correction, cluster $p < .05$, voxel $p < .001$). In the secondary seed-based FC analysis, the same statistical analyses as for ALFF were employed to explore the network involved in MCI in MSA patients. The whole-brain GM volumes obtained from VBM analysis were also compared among the three groups, and post hoc analysis was further performed between patient groups, with the TIV added into covariates (GRF correction, cluster $p < .05$, voxel $p < .001$).

3 | RESULTS

3.1 | Demographics and clinical data

The demographics and clinical data of the three groups are presented in Table 1. A total of 120 subjects were included in the current study, of whom 44 were MSA-MCI, 36 were MSA-NC, and 40 were HC. There were no significant between-group differences in age, gender, or education among the three groups. MSA-MCI patients showed significantly lower MoCA and MMSE scores than MSA-NC patients and HCs. There were no significant differences in disease duration, H–Y stage, UMSARS-II scores, or levodopa equivalent dose between patient groups.

3.2 | ALFF analysis

Compared with HCs, the MSA-MCI group showed decreased ALFF in the bilateral middle frontal gyrus (MFG), superior frontal gyrus, medial superior frontal gyrus, supplementary motor area, precentral gyrus, right inferior frontal gyrus (IFG), and precuneus and increased ALFF in the right cerebellum. The MSA-NC group showed decreased ALFF in the bilateral medial superior frontal gyrus, MFG, and superior frontal gyrus. When directly compared with MSA-NC, the MSA-MCI group

TABLE 1 Demographics and clinical data of all participants

Characteristics	HC ($n = 40$)	MSA-NC ($n = 36$)	MSA-MCI ($n = 44$)	Analysis	
				χ^2/z	p
Age (years)	64.00 (61.00, 67.00)	61.00 (56.00, 65.50)	65.00 (61.50, 68.50)	5.493	.064
Gender (male/female)	16/24	19/17	20/24	1.250	.535
Education (years)	12.00 (9.00, 15.00)	12.00 (9.00, 15.00)	11.00 (9.00, 12.00)	5.318	.070
MoCA score	27.00 (26.00, 28.00)	26.00 (25.00, 28.00)	21.00 (19.00, 23.00)	84.643	.000
MMSE score	30.00 (29.00, 30.00)	28.00 (27.00, 29.00)	26.00 (25.00, 27.00)	52.897	.000
HAMD-24 score	4.00 (3.00, 6.00)	7.00 (6.00, 8.00)	7.00 (6.00, 8.00)	34.090	.000
Disease duration (years)	-	3.00 (2.00, 4.00)	2.25 (2.00, 3.75)	−0.863	.388
H–Y	-	2.00 (1.50, 3.00)	2.00 (2.00, 3.00)	−0.508	.611
UMSARS-II score	-	12.50 (7.00, 16.50)	12.5 (7.00, 17.00)	−0.242	.809
LEDD (mg/day)	-	300.00 (174.75, 599.25)	337.50 (200.00, 525.00)	−0.121	.904

Note: Continuous variables distributed non-normally are expressed as median (interquartile range [IQR]), while categorical variable is presented with number of patients. χ^2-values were obtained using a chi-square test. *z*-Values were obtained using Mann–Whitney *U* test. $p < .05$ was considered statistically significant.

Abbreviations: HAMD, Hamilton Depression Scale; HC, healthy controls; H–Y, Hoehn and Yahr stage; LEED, levodopa equivalent dose; MMSE, Mini-Mental State Examination; MoCA, Montreal Cognitive Assessment; MSA-MCI, multiple system atrophy patients with mild cognitive impairment; MSA-NC, multiple system atrophy patients with normal cognition; *n*, number of subjects; UMSARS-II, Unified Multiple System Atrophy Rating Scale-Part II.

TABLE 2 Differences in the ALFF values between MSA patients and HCs

Brain regions	Cluster size, voxels	Peak MNI coordinate			*t* value
		x	*y*	*z*	
MSA-MCI versus HC					
Cerebelum_8/9_R	263	21	−54	−51	6.2881
Cerebelum_4_5_R	55	30	−42	−24	4.9616
Frontal_Mid_R	507	39	39	21	−6.0873
Frontal_Inf_Tri/Oper_R					
Frontal_Sup_R					
Precentral_R					
Frontal_Mid_L	959	−27	30	48	−6.5913
Frontal_Sup_L					
Frontal_Sup_Medial_L/R					
Supp_Motor_Area_L/R					
Precentral_L					
Precuneus_R	27	24	−63	27	5.5345
Frontal_Sup_R	29	24	30	51	−5.6767
MSA-NC versus HC					
Frontal_Sup_Medial_L/R	67	0	36	48	−3.8448
Frontal_Mid_L	24	−33	27	45	−3.8581
Frontal_Mid_R	29	33	30	48	−4.2654
Frontal_Sup_L	94	−21	−3	66	−4.3907
Frontal_Sup_R	25	21	27	57	−4.0361
MSA-MCI versus MSA-NC					
Cerebelum_9_R	103	18	−48	−48	4.3064
Cerebelum_8_R					
Cerebellum_4_5_R	40	27	−45	−21	4.152
Fusiform_R					
Frontal_Mid_R	245	42	33	15	−5.4578
Frontal_Inf_Tri_R					
Frontal_Inf_Oper_R					

Note: *x*, *y*, *z* are the coordinates of primary peak locations in the MNI space. The negative *t* value represents decreased ALFF and the positive *t* value represents increased ALFF.
Abbreviations: ALFF, amplitude of low-frequency fluctuation; Cerebelum_4_5/8/9, cerebellar lobule IV/V, VIII, IX; Frontal_Inf_Oper, the opercular part of the inferior frontal gyrus; Frontal_Inf_Tri, the triangular part of the inferior frontal gyrus; Frontal_Mid, middle frontal gyrus; Frontal_Sup, superior frontal gyrus; HC, healthy controls; L, left; MNI, Montreal Neurological Institute; MSA-MCI, multiple system atrophy patients with mild cognitive impairment; MSA-NC, multiple system atrophy patients with normal cognition; R, right; Supp_Motor_Area, supplementary motor area.

showed decreased ALFF in the RDLPFC, including the right MFG, and right opercular and triangular parts of the IFG, and increased ALFF in the right cerebellum, including rCbe9 and rCbe4-5 (Table 2 and Figures 1 and 2a).

3.3 | Seed-based FC analysis

3.3.1 | RDLPFC related FC alteration

Compared with HCs, the MSA-MCI group showed decreased RDLPFC-based FC in the bilateral cerebellum, left IFG, bilateral inferior parietal lobe (IPL), bilateral precentral gyrus, right angular gyrus, and bilateral MFG. The MSA-NC group showed decreased FC in the bilateral cerebellum, left IFG, right precentral gyrus, and right MFG. Only the left IPL showed significant RDLPFC-based FC changes between MSA-MCI and MSA-NC patients (Table 3 and Figures 3a and 4a,b).

3.3.2 | Right cerebellum related FC alteration

Compared with HC, with rCbe9 as the seed, MSA-MCI patients showed decreased FC in the left superior parietal gyrus, IFG,

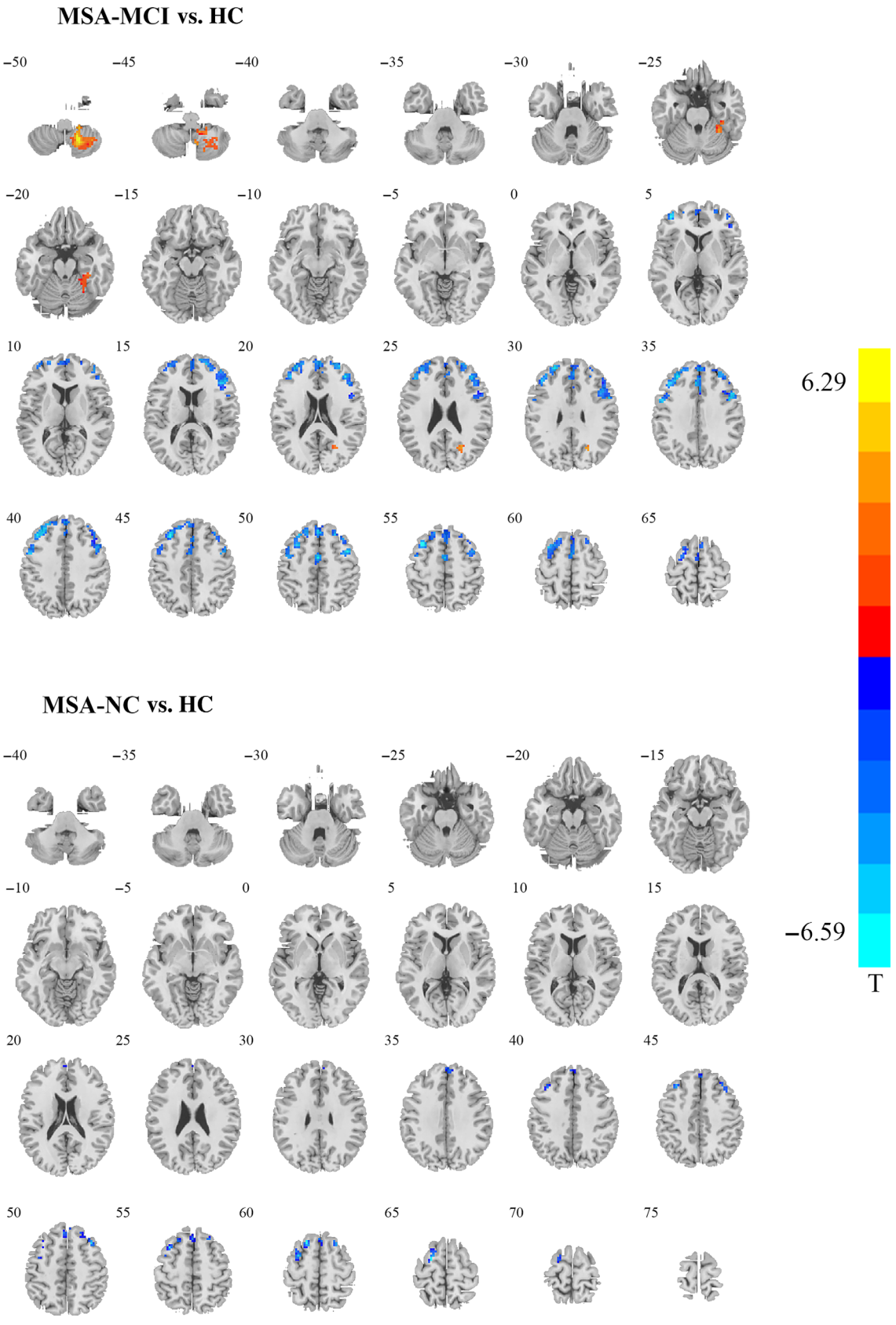

FIGURE 1 Statistical maps showing amplitude of low-frequency fluctuation (ALFF) differences in the patient groups relative to healthy controls. The left side of the image corresponds to the left side of the brain in axial orientation. Slice coordinates according to the Montreal Neurological Institute space are shown on the upper left corner of the slices, indicating the *z* axis in axial orientation. The *t*-value scale is seen to the right of the image. Red and blue denote higher and lower ALFFs, respectively. $p < .05$, Gaussian random field corrected

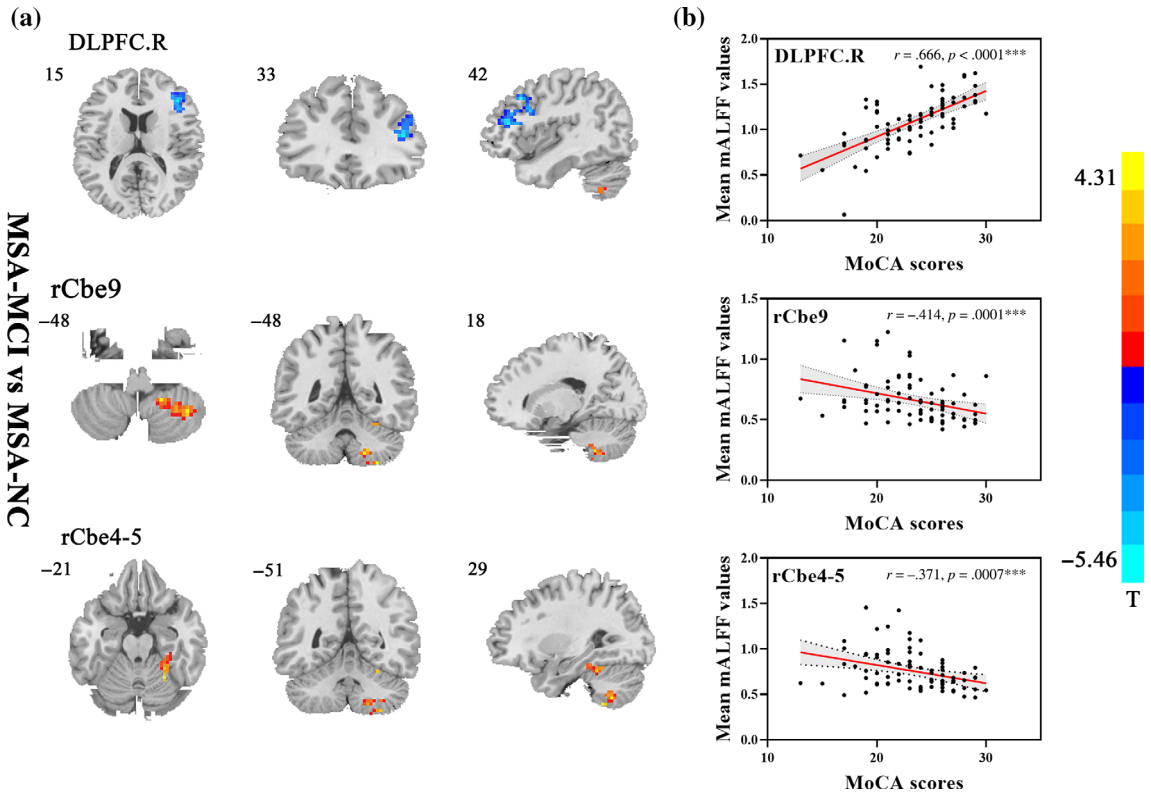

FIGURE 2 Brain areas showing amplitude of low-frequency fluctuation (ALFF) differences between the multiple system atrophy patients with mild cognitive impairment (MSA-MCI) and the multiple system atrophy patients with normal cognition (MSA-NC) group (a), and correlations between mean mALFF values and Montreal Cognitive Assessment (MoCA) scores in MSA patients (b). (a) Blue represents lower ALFF in the right dorsal lateral prefrontal cortex, and red represents higher ALFF in the right cerebellar lobule IX and lobule IV–V. $p < .05$, Gaussian random field corrected. (b) There was a positive correlation between the mALFF values of the right dorsal lateral prefrontal cortex and the MoCA scores of MSA patients. There was a negative correlation between the mALFF values of the right cerebellum and the MoCA scores of MSA patients. ***$p < .001$. DLPFC.R, the right dorsal lateral prefrontal cortex; rCbe9, the right cerebellar lobule IX; rCbe4-5, the right cerebellar lobule IV–V

precuneus, bilateral middle occipital gyrus, cuneus, and superior occipital gyrus. MSA-NC patients showed decreased FC in the right middle temporal gyrus (MTG) and inferior temporal gyrus. When directly compared with MSA-NC, MSA-MCI patients showed decreased FC in the bilateral cuneus, left precuneus, and IPL and increased FC in the right MTG (Table 3 and Figures 3b and 5a,b).

With rCbe4-5 as the seed region, MSA-MCI and MSA-NC patients showed similar decreased FC regions in the left parahippocampal gyrus, IPL, postcentral gyrus, supramarginal gyrus, right putamen, insula, middle cingulum gyrus, and bilateral insula. There were no significant alterations when directly comparing MSA-MCI with MSA-NC patients.

3.4 | VBM analysis

Compared with HCs, both MSA patient groups showed volume reduction in bilateral cerebellum, vermis, bilateral temporal and occipital lobe, bilateral putman, and bilateral fusiform gyrus, of which MSA-MCI patients exhibited more widespread alterations. However, no significant volume reduction was detected between patient groups (Table S1 and Figures 1 and 2).

3.5 | Correlation analysis of ALFF and FC changes with clinical scores in patient groups

Since the MoCA scale shows higher validity than the MMSE in the detection of MCI (Fiorenzato et al., 2016; Hoops et al., 2009), we selected MoCA scores for cognitive correlation analyses. Figures 2b, 4c, and 5c show scatter plots for correlation analyses of ALFF and FC alterations with MoCA scores in patient groups. In MSA patients, mALFF values in the RDLPFC were negatively correlated with MoCA scores ($r = .67$, $p < .0001$), while mALFF values in the right cerebellum were positively correlated with MoCA scores (rCbe9: $r = .41$, $p = .0001$; rCbe4-5: $r = .37$, $p = .0007$) (Figure 2b).

In FC analysis, zFC values of the RDLPFC and the left IPL were positively correlated with MoCA scores ($r = .365$, $p = .009$) in MSA patients. With rCbe9 as the seed region, the FC of rCbe9 and the bilateral cuneus ($r = .244$, $p = .0293$), left precuneus ($r = .363$, $p = .0009$), and left IPL ($r = .386$, $p = .0004$) were positively correlated with MoCA scores, while rCbe9-right MFG ($r = -.275$, $p = .0135$) was negatively correlated with MoCA scores (Figures 4c and 5c).

No significant correlation was shown with other clinical scores in MSA patients (see Table S2).

TABLE 3 FC differences between patient groups and HCs when considering the right dorsal lateral prefrontal cortex and the right cerebellar lobule IX as the seed regions for whole-brain voxels

Brain regions	Cluster size, voxels	Peak MNI coordinate			*t* value
		x	*y*	*z*	
The right dorsal lateral prefrontal cortex as the seed region					
MSA-MCI versus HC					
Cerebelum_6/Crus1/Crus2_L/R, Vermis_4_5/Vermis_6, Cerebelum_7b/8_R	535	12	−72	−30	−6.1368
Frontal_Inf_Tri/Orb_L	75	−39	30	0	−4.8652
Parietal_Inf_L	352	−30	−75	45	−5.5273
Precentral_R, Frontal_Mid_R	138	30	−3	45	−4.798
Angular_R, Occipital_Mid_R, Parietal_Inf_R	125	36	−69	33	−4.7421
Frontal_Mid_L	47	−45	9	36	−5.0167
Precentral_L	52	−33	−9	48	−4.8232
MSA-NC versus HC					
Cerebelum_Crus2_R	59	12	−78	−33	−4.689
Cerebelum_6_R	37	9	−60	−21	−3.5079
Cerebelum_6_L	69	−30	−57	−21	−4.6259
Frontal_Inf_Orb/Tri_L	46	−39	30	−3	−4.4461
Precentral_R	94	42	3	33	−4.3389
Frontal_Mid_R					
MSA-MCI versus MSA-NC					
Parietal_Inf_L	60	−33	−51	33	−3.8779
Angular_L					
The right cerebellar lobule IX as the seed region					
MSA-MCI versus HC					
Parietal_Sup/Inf_L, Occipital_Sup/Mid_L/R, Cuneus_L/R, Precuneus_L	351	30	−78	27	−4.8378
MSA-NC versus HC					
Temporal_Mid/Inf_R	73	51	−15	−24	−4.6206
MSA-MCI versus MSA-NC					
Temporal_Mid_R	19	51	−6	−12	4.0137
Cuneus_L/R	46	−3	−75	15	−3.803
Precuneus_L	52	−15	−66	42	−4.5192
Parietal_Inf_L	19	−24	−48	42	−4.0901

Note: *x*, *y*, *z* are the coordinates of primary peak locations in the MNI space. The negative *t* value represents decreased FC and the positive *t* value represents increased FC.

Abbreviations: Cerebelum_4_5/6/7b/8/9/Crus1/Crus2, cerebellar lobule IV/V, VI, VIIb, VIII, IX, Crus I, Crus II; Frontal_Inf_Orb, the orbital part of the inferior frontal gyrus; Frontal_Inf_Tri, the triangular part of the inferior frontal gyrus; Frontal_Mid, middle frontal gyrus; HC, healthy controls; L, Left; MNI, Montreal Neurological Institute; MSA-MCI, multiple system atrophy patients with mild cognitive impairment; MSA-NC, multiple system atrophy patients with normal cognition; Occipital_Mid_R, middle occipital gyrus; Occipital_Sup, superior occipital gyrus; Parietal_Inf, inferior parietal lobe; Parietal_Sup, superior parietal lobe; R, Right; Temporal_Inf, inferior temporal gyrus; Temporal_Mid, middle temporal gyrus.

4 | DISCUSSION

We combined ALFF, seed-based FC, and VBM analyses in MSA-MCI, MSA-NC, and healthy controls. First, compared to MSA-NC, MSA-MCI showed cognition-related local deactivation in the right dorsal lateral prefrontal cortex (DLPFC), and decreased FC between the right DLPFC and the left IPL. Second, MSA-MCI exhibited cognition-related local activation in the right cerebellum compared to MSA-NC. With the right cerebellar lobule IX (rCbe9) as the seed, we found decreased FC in the left precuneus, IPL, and bilateral cuneus, and increased FC in the right MTG. Third, we found no GM volume reduction between MSA-MCI and MSA-NC. These findings confirmed our hypotheses that degeneration in the DLPFC and cerebellum, as well as corresponding disruption in the DLPFC-IPL and cerebello-cerebral networks, might be simultaneously involved in early cognitive decline in MSA.

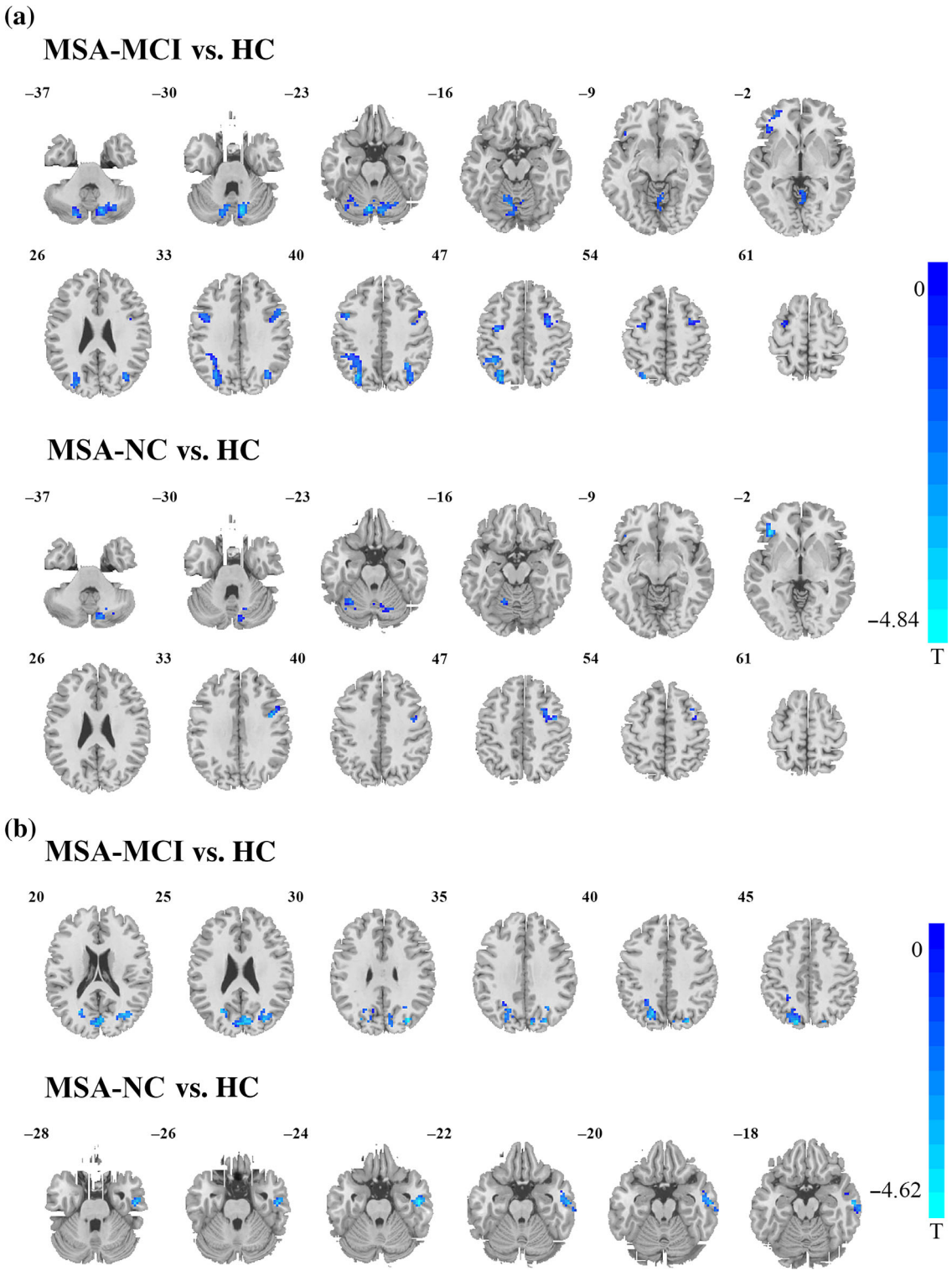

FIGURE 3 Brain regions showing differences in functional connectivities, considering the right dorsal lateral prefrontal cortex (a) and the right cerebellar lobule IX (b) as the seed regions for whole-brain voxels, between the patient groups and healthy controls. $p < .05$, Gaussian random field corrected.

In MSA, CI prominently occurs in the frontal executive domain (Brown et al., 2010; Elliott, 2003), and the prefrontal lobe, especially the DLPFC, has been confirmed to be closely related to executive function (Breukelaar et al., 2017; Godefroy, 2003). Post-mortem evidence has revealed that fewer neurons in the frontal cortex was correlated with CI in MSA patients (Salvesen et al., 2017), and the DLPFC has been reported to show functional and morphological abnormalities related to CI in MSA patients, such as volume reduction

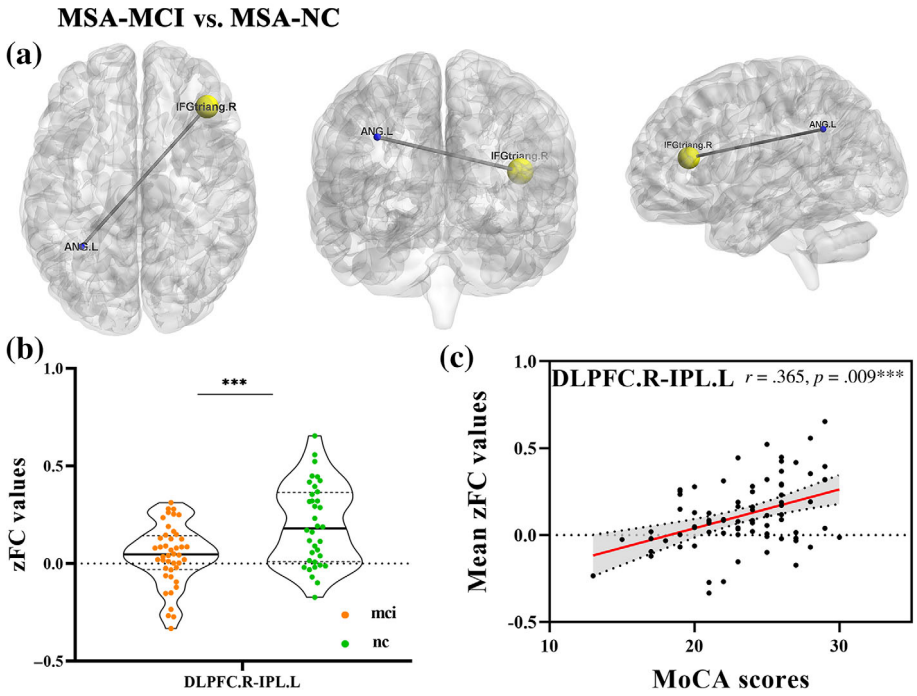

FIGURE 4 Seed-based functional connectivity (FC) maps with right dorsal lateral prefrontal cortex as the seed in a comparison of the multiple system atrophy patients with mild cognitive impairment (MSA-MCI) and multiple system atrophy patients with normal cognition (MSA-NC) groups based on resting-state functional magnetic resonance imaging (a and b), and correlations between mean zFC values and Montreal Cognitive Assessment (MoCA) scores in MSA patients (c). (a) Compared to the MSA-NC group, the MSA-MCI group showed decreased FC between right dorsal lateral prefrontal cortex and the left IPL. $p < .05$, Gaussian random field corrected. (b) Violin plots show the data distribution of zFC values within the MSA-MCI and MSA-NC groups. The solid line represents the median, and the dotted line represents the 25th and 75th percentiles of each data set. (c) There was a positive correlation between the zFC values of the DLPFC.R-IPL.L and the MoCA scores of MSA patients. ***$p < .001$. ANG_L, the left angular gyrus; DLPFC.R, the right dorsal lateral prefrontal cortex; IFGtriang_R, the right triangular part of the inferior frontal gyrus; IPL.L, the left inferior parietal lobe

(Fiorenzato et al., 2017), hypoperfusion (Kawai et al., 2008), and decreased centrality level (Yang et al., 2020). Our findings showed decreased ALFF in the right DLPFC regions, indicating decreased focal spontaneous activity of the DLPFC in MSA-MCI, further confirming the critical role the DLPFC plays in the cognitive deficits of MSA patients.

Moreover, we found decreased FC between the right DLPFC and the left IPL. An [18F]-deoxyglucose (FDG) PET study has reported that hypometabolism in MSA begins in the frontal lobe and spreads to the parieto-temporal lobe, and the process coincides with the cognitive decline (Lyoo et al., 2008). This is consistent with our finding that decreased spontaneous activity in the DLPFC and corresponding disconnection with the IPL were involved in MSA-MCI. The IPL supports an extensive range of cognitive functions, including visuospatial attention, memory, motor planning, and mathematical cognition (Uddin et al., 2010). The left IPL, vital for the storage of visual short-term memory (Chen et al., 2021; Henson et al., 2000; Todd & Marois, 2004), is considered a promising biomarker to distinguish aMCI from HC (Hänggi et al., 2011). Particularly, the peak MNI coordinate of IPL in our study was located in the angular gyrus. Cortical thinning in the posterior brain regions, particularly the left angular gyrus, as well as frontal regions were selected as significant predictors of conversion from PD with MCI to PDD (Shin et al., 2021). In MSA patients, our results suggest the early cognitive decline may be caused by the degeneration of RDLPFC and dysfunction of the DLPFC-IPL connection. The DLPFC and IPL regions in our study mostly overlap with the executive control network (ECN), which is anchored in DLPFC and posterior parietal lobe. Our results indicated that the disconnection in ECN was involved in MSA-MCI. In ECN, the DLPFC and IPL are functionally coupled in higher-order executive control, especially in maintaining and manipulating information of the working memory and decision making in goal-directed processing (Menon, 2015; Seeley et al., 2007). ECN disruption is widespread in psychiatric and neurological disorders, including depression, AD, schizophrenia, and PD, but this has not been discussed in MSA (Menon, 2011; Tang et al., 2022). Our findings indicated ECN disruption induced by DLPFC-IPL disconnection may be related to dysfunction in working memory and top-down control in MSA patients.

Another brain region with altered ALFF is the right cerebellum. Cerebellar degeneration is well known in MSA (Jellinger et al., 2005). However, it has long been associated with motor function. Emerging evidence has led to new insights into the role of the cerebellum in cognitive modulation (Buckner, 2013; Minnerop et al., 2007; Strick et al., 2009). Dysfunction in the cerebellum, especially in the posterior

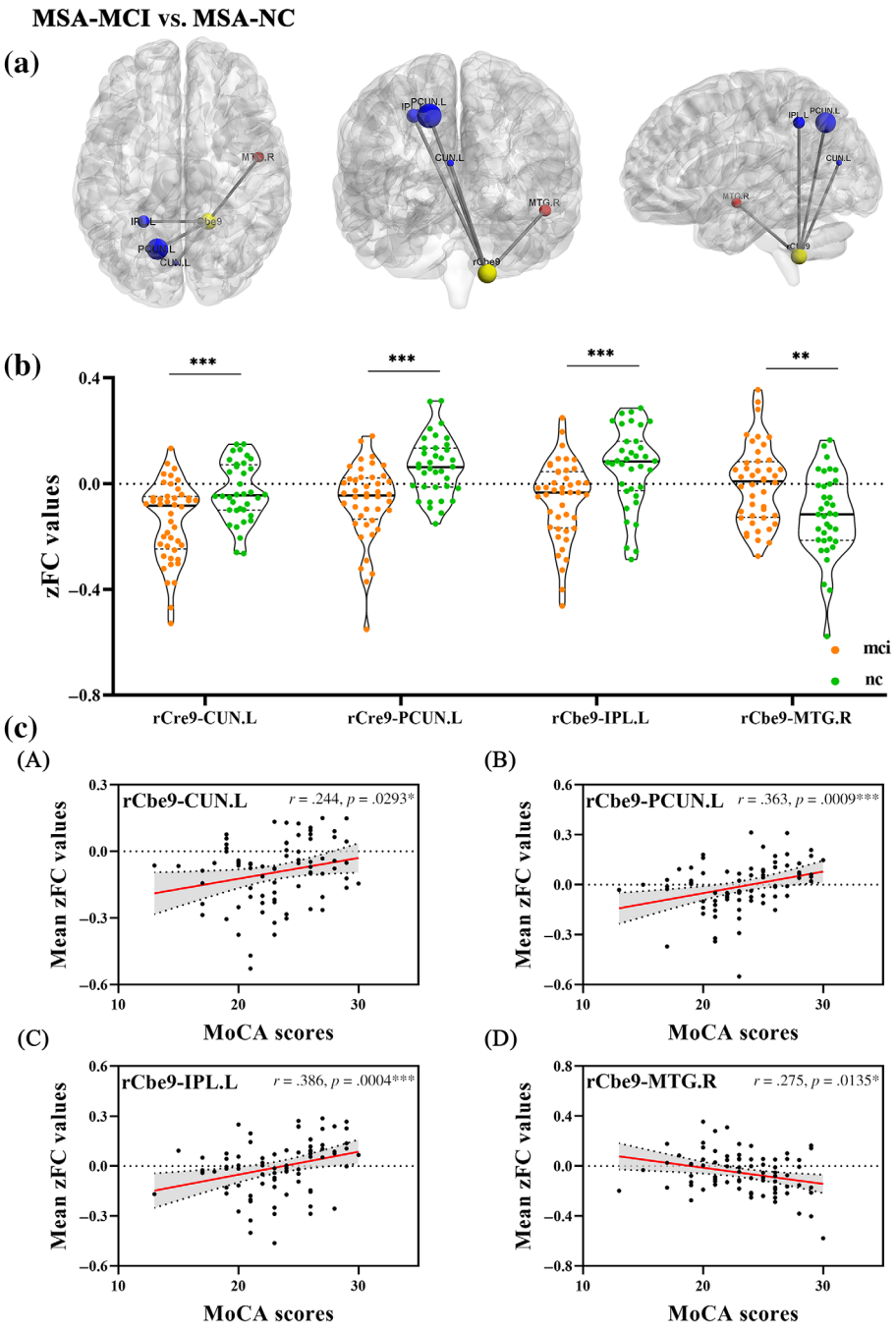

FIGURE 5 Seed-based functional connectivity (FC) maps with right cerebellar lobule IX as the seed in a comparison of the multiple system atrophy patients with mild cognitive impairment (MSA-MCI) and multiple system atrophy patients with mild cognitive impairment (MSA-NC) groups based on resting-state functional magnetic resonance imaging (a and b), and correlations between mean zFC values and Montreal Cognitive Assessment (MoCA) scores in MSA patients (c). (a) Compared to the MSA-NC group, the MSA-MCI group showed decreased FC between right cerebellar lobule IX and the bilateral cuneus, left precuneus, and left inferior parietal lobe and increased FC in the right middle temporal gyrus. $p < .05$, Gaussian random field corrected. (b) Violin plots show the data distribution of zFC values within the MSA-MCI and MSA-NC groups. The solid line represents the median, and the dotted line represents the 25th and 75th percentiles of each data set. (a) There was a positive correlation between the zFC values of the rCbe9–CUN.L and the MoCA scores of MSA patients. (b) There was a positive correlation between the zFC values of the rCbe9–PCUN.L and the MoCA scores of MSA patients. (b) There was a positive correlation between the zFC values of the rCbe9–IPL.L and the MoCA scores of MSA patients. (d) There was a negative correlation between the zFC values of the rCbe9–MTG.R and the MoCA scores of MSA patients. *$p < .05$; **$p < .01$; ***$p < .001$. CUN.L, the left cuneus; IPL.L, the left inferior parietal lobe; MTG.R, the right middle temporal gyrus; PCUN.L, the left precuneus; rCbe9, the right cerebellar lobule IX

lobe, may contribute to cerebellar cognitive affective syndrome (Schmahmann & Sherman, 1998), characterized by deficits in spatial cognition, linguistic skills, emotional processing and disturbances of executive functions. [18F]-FDG-PET studies indicated that hypometabolism of the cerebellum occurred in the early stage of MSA (Lyoo et al., 2008), and the metabolic changes were correlated with attention, language, and visuospatial and executive function (Shen et al., 2022). Our previous Spatially Unbiased Infratentorial Template (SUIT)-VBM findings validated that the volumetric alterations of the posterior cerebellum contribute to the cognitive performance in MSA patients (Yang, Wang, Luo, Lv, Liu, Li, & Fan, 2019b). Most studies have suggested that the cerebellum plays a pathological role in CI in MSA (Kawabata et al., 2019; Wang et al., 2017; Yang, Wang, Luo, Lv, Liu, Li, & Fan, 2019b), while in our study, increased ALFF reflected activation in the cerebellum, indicating a compensatory role. Besides, the ALFF values were negatively correlated with cognitive scores. In other words, increased spontaneous activity was related to poor performance in cognition. We hypothesized that the spontaneous neuronal activity in the cerebellum would be strengthened to maintain cognitive performance but fail, since the compensatory mechanism would collapse, and would subsequently enter a decompensatory stage. The gradual disturbance was also documented in the

Alzheimer's spectrum (Yang et al., 2018), reflecting the impending neuronal network breakdown as cognition declines as a result of the worsening local and global neurodegenerative pathology.

The theory of the universal cerebellar transform states that lesions of the posterior lobe of the cerebellum influence multiple non-motor areas in the cortices through cerebrocerebellar projections, thus producing cognitive and emotional symptoms (Schmahmann et al., 2019; Strick et al., 2009). In our study, with the rCbe9 as the seed, we found decreased FC in the left precuneus, IPL, and bilateral cuneus as well as increased FC in the right MTG. These were correlated with MoCA scores, indicating the disruption of the cerebello-cerebral circuit may play a role in the CI in MSA. A previous study (Kawabata et al., 2019) documented cognitive-related cerebello-cerebral network interruption in MSA, lying in the cerebello-medial prefrontal and cerebello-amygdaloid circuit. The medial prefrontal lobe is part of the dorsal default mode network (dDMN), but the cortical regions with decreased FC observed in our study were located in the posterior DMN (pDMN). The dDMN is associated with self-referential mental activity, whereas the pDMN is the structural core of DMN subsystems important for functional integration, supporting the recollection of prior experiences (Buckner & DiNicola, 2019; Raichle, 2015). The pDMN dysfunction serves an important role in cognitive dysfunction in AD (Ibrahim et al., 2021; Jones et al., 2011; Mandal et al., 2018). A longitudinal study (Damoiseaux et al., 2012) in AD patients showed the decreased FC in pDMN at the baseline whereas the initially increased FC within the ventral and anterior DMN, both subsequently declining as the disease progressed. Furthermore, another study (Jones et al., 2016) of DMN subsystems revealed that network failure across AD spectrum began with a decline in the most highly connected pDMN, followed by the transient increase in connectivity related to other subsystems. Rather than the compensatory phenomenon, the increased connectivity may be the sign of high processing burden that may eventually lead to widespread system failure. Similarly in our study, decreased cerebellar FC was shown in pDMN related to early cognitive decline in MSA-MCI, whereas increased cerebellar FC in the right MTG, negatively correlated with cognitive performance. Our results suggested that shared network disruption in DMN may be present in MSA-MCI and early AD, which need further investigation.

ECN is engaged in external oriented and goal-directed processes, whereas DMN focuses on monitoring the internal mental landscape. The integrity of ECN and DMN, and the dynamic switching and balancing between them appear fundamental to the promotion of efficient cognitive processing in healthy individuals (Menon, 2011; Ng et al., 2016). The disruption of ECN and DMN has been associated with processing speed, executive control, episodic memory, and working memory (Andrews-Hanna et al., 2007; Ng et al., 2016). The idea that it may play a role in PD, autism, auditory hallucinations, or AD has been discussed (Menon, 2011; Putcha et al., 2015), but it remains to be determined in MSA. Our results indicated functional disconnection in ECN in MSA. The cerebellum makes an effort to compensate for the abnormality through the cerebello-cerebral circuit but it fails, contributing to functional disruptions in DMN. We speculate the aberrant crosstalk between ECN and DMN underlies the cognitive decline in MSA, and the cerebellum modulates this process. Our results suggest inappropriate assignment between goal-related and goal-irrelevant information, providing new insight into aberrant brain organization in ECN, DMN, and the cerebellum in MSA-MCI.

Our VBM analysis showed no differences in GM volume between the two patient subgroups, which is inconsistent with our functional findings, suggesting that functional disruptions, rather than structural alterations, contribute to MCI in MSA. Cognition-related changes in neuronal activity precede structural changes in MSA-MCI. Besides, the patient groups showed no volume reduction in the frontal cortices, indicating that the MSA-MCI patients in our study are in the early stage of CI. This is consistent with our original research settings. Nevertheless, several prior studies have reported structural changes in MSA that contribute to CI. The discrepancies between the previous studies and ours might lie in the different research design (MSA [Kawabata et al., 2019], MSA-C [Lee et al., 2016], and MSA-P [Kim et al., 2015] compared with HC in prior research vs. direct comparison between patients with and without MCI in ours), different severities of CI (MMSE scores of 21.91 ± 2.31 in MSA-CI in a prior study [Yang et al., 2020] vs. 26.32 ± 1.78 in ours, 26.7 ± 3.1 in the MSA group in another study [Fiorenzato et al., 2017] vs. 27.24 ± 1.84 in ours), and heterogeneity in patient samples. Our findings provide new insights into the mechanism underlying the conversion from normal cognition to early cognitive decline in MSA patients. Within existing literature, Kawabata et al. (2019) held the view that CI in MSA was caused by cerebellum degeneration and subcortical network dysfunction. Fiorenzato et al. (2017) believed that cortical pathology in MSA-CI was driven by subcortical degeneration via the frontostriatal circuit. Meanwhile, Cao et al. (2021) proposed that cortical thinning in the left MTG primarily contributed to cognitive deficits in MSA. Our results indicated that cerebellar degeneration and corresponding cortical abnormalities, as well as primary cortical network dysfunction, might simultaneously contribute to MCI in MSA, and early cognitive decline in MSA is more dependent on functional disruptions than on morphological changes.

There are some limitations to our study. First, we only examined global cognition using MMSE and MoCA scales. No domain-specific assessments were employed, and we could not identify the brain functional alteration patterns in a specific cognitive domain. Second, many MSA patients take antiparkinsonian medications as well as antidepressants as daily treatments, which may influence their brain activity. Although we asked participants to undergo medication withdrawal at least 12 h prior to the scan, the potential influence cannot be excluded. Third, this was a cross-sectional study, and we were unable to detect the temporal transformation of brain function. We have already added comprehensive neuropsychological examinations in our ongoing studies. Finally, the age difference among the groups ($p = .064$) was not statistically significant, but it does not mean there was no difference. The marginally significant difference may have a potential impact on cognition. Although age was regressed out in the study, we should take the effect into account. Future studies should focus on the relationship between cognition-specific domains and brain functional changes. Longitudinal studies, the inclusion of more non medicated participants, and better matching between groups should also be considered.

5 | CONCLUSION

Our results indicated that MCI in MSA was related to hypo-activation of the right DLPFC and corresponding DLPFC-IPL network dysfunction as well as hyper-activation of the right cerebellum and corresponding cerebello-DMN network disruption. Furthermore, we found no GM atrophy between MSA-MCI and MSA-NC, suggesting early cognitive decline in MSA patients is more attributable to functional changes than to anatomical damage. In conclusion, our findings provide a further understanding that primary cortical damage and subcortical degeneration with secondary cortical deafferentation might simultaneously contribute to early cognitive decline in MSA.

ACKNOWLEDGMENT

This work was supported by research grants from the National Natural Science Foundation of China (82071909).

CONFLICT OF INTEREST

The authors declare no potential conflict of interest.

DATA AVAILABILITY STATEMENT

The data that support the findings of this study are available from the corresponding author upon reasonable request.

ORCID

Guoguang Fan https://orcid.org/0000-0001-8114-5727

REFERENCES

Andrews-Hanna, J. R., Snyder, A. Z., Vincent, J. L., Lustig, C., Head, D., Raichle, M. E., & Buckner, R. L. (2007). Disruption of large-scale brain systems in advanced aging. *Neuron*, *56*(5), 924–935. https://doi.org/10.1016/j.neuron.2007.10.038

Biswal, B. B. (2012). Resting state fMRI: A personal history. *NeuroImage*, *62*(2), 938–944. https://doi.org/10.1016/j.neuroimage.2012.01.090

Breukelaar, I. A., Antees, C., Grieve, S. M., Foster, S. L., Gomes, L., Williams, L. M., & Korgaonkar, M. S. (2017). Cognitive control network anatomy correlates with neurocognitive behavior: A longitudinal study. *Human Brain Mapping*, *38*(2), 631–643. https://doi.org/10.1002/hbm.23401

Brown, R. G., Lacomblez, L., Landwehrmeyer, B. G., Bak, T., Uttner, I., Dubois, B., Agid, Y., Ludolph, A., Bensimon, G., Payan, C., Leigh, N. P., & NNIPPS Study Group. (2010). Cognitive impairment in patients with multiple system atrophy and progressive supranuclear palsy. *Brain*, *133*(Pt 8), 2382–2393. https://doi.org/10.1093/brain/awq158

Buckner, R. L. (2013). The cerebellum and cognitive function: 25 years of insight from anatomy and neuroimaging. *Neuron*, *80*(3), 807–815. https://doi.org/10.1016/j.neuron.2013.10.044

Buckner, R. L., & DiNicola, L. M. (2019). The brain's default network: Updated anatomy, physiology and evolving insights. *Nature Reviews Neuroscience*, *20*(10), 593–608. https://doi.org/10.1038/s41583-019-0212-7

Cai, S., Chong, T., Peng, Y., Shen, W., Li, J., von Deneen, K. M., L, H., & Alzheimer's Disease Neuroimaging Initiative. (2017). Altered functional brain networks in amnestic mild cognitive impairment: A resting-state fMRI study. *Brain Imaging and Behavior*, *11*(3), 619–631. https://doi.org/10.1007/s11682-016-9539-0

Cao, C., Wang, Q., Yu, H., Yang, H., Li, Y., Guo, M., Huo, H., & Fan, G. (2021). Morphological changes in cortical and subcortical structures in multiple system atrophy patients with mild cognitive impairment. *Frontiers in Human Neuroscience*, *15*, 649051. https://doi.org/10.3389/fnhum.2021.649051

Caso, F., Canu, E., Lukic, M. J., Petrovic, I. N., Fontana, A., Nikolic, I., Kostic, V. S., Filippi, M., & Agosta, F. (2020). Cognitive impairment and structural brain damage in multiple system atrophy-parkinsonian variant. *Journal of Neurology*, *267*(1), 87–94. https://doi.org/10.1007/s00415-019-09555-y

Chang, C. C., Chang, Y. Y., Chang, W. N., Lee, Y. C., Wang, Y. L., Lui, C. C., Huang, C. W., & Liu, W. L. (2009). Cognitive deficits in multiple system atrophy correlate with frontal atrophy and disease duration. *European Journal of Neurology*, *16*(10), 1144–1150. https://doi.org/10.1111/j.1468-1331.2009.02661.x

Chen, P. Y., Hsu, H. Y., Chao, Y. P., Nouchi, R., Wang, P. N., & Cheng, C. H. (2021). Altered mismatch response of inferior parietal lobule in amnestic mild cognitive impairment: A magnetoencephalographic study. *CNS Neuroscience & Therapeutics*, *27*(10), 1136–1145. https://doi.org/10.1111/cns.13691

Cykowski, M. D., Coon, E. A., Powell, S. Z., Jenkins, S. M., Benarroch, E. E., Low, P. A., Schmeichel, A. M., & Parisi, J. E. (2015). Expanding the spectrum of neuronal pathology in multiple system atrophy. *Brain*, *138*(Pt 8), 2293–2309. https://doi.org/10.1093/brain/awv114

Damoiseaux, J. S., Prater, K. E., Miller, B. L., & Greicius, M. D. (2012). Functional connectivity tracks clinical deterioration in Alzheimer's disease. *Neurobiology of Aging*, *33*(4), 828.e19–828.e30. https://doi.org/10.1016/j.neurobiolaging.2011.06.024

Dubois, B., Burn, D., Goetz, C., Aarsland, D., Brown, R. G., Broe, G. A., Dickson, D., Duyckaerts, C., Cummings, J., Gauthier, S., Korczyn, A., Lees, A., Levy, R., Litvan, I., Mizuno, Y., McKeith, I. G., Olanow, C. W., Poewe, W., Sampaio, C., … Emre, M. (2007). Diagnostic procedures for Parkinson's disease dementia: Recommendations from the movement disorder society task force. *Movement Disorders*, *22*(16), 2314–2324. https://doi.org/10.1002/mds.21844

Elliott, R. (2003). Executive functions and their disorders. *British Medical Bulletin*, *65*, 49–59. https://doi.org/10.1093/bmb/65.1.49

Fiorenzato, E., Antonini, A., Wenning, G., & Biundo, R. (2017). Cognitive impairment in multiple system atrophy. *Movement Disorders*, *32*(9), 1338–1339. https://doi.org/10.1002/mds.27085

Fiorenzato, E., Weis, L., Falup-Pecurariu, C., Diaconu, S., Siri, C., Reali, E., Pezzoli, G., Bisiacchi, P., Antonini, A., & Biundo, R. (2016). Montreal Cognitive Assessment (MoCA) and Mini-Mental State Examination (MMSE) performance in progressive supranuclear palsy and multiple system atrophy. *Journal of Neural Transmission*, *123*(12), 1435–1442. https://doi.org/10.1007/s00702-016-1589-3

Fiorenzato, E., Weis, L., Seppi, K., Onofrj, M., Cortelli, P., Zanigni, S., Tonon, C., Kaufmann, H., Shepherd, T. M., Poewe, W., Krismer, F., Wenning, G., Antonini, A., Biundo, R., & Movement Disorders Society MSA (MODIMSA) Neuropsychology and Imaging Study Groups. (2017). Brain structural profile of multiple system atrophy patients with cognitive impairment. *Journal of Neural Transmission*, *124*(3), 293–302. https://doi.org/10.1007/s00702-016-1636-0

Friston, K. J. (2011). Functional and effective connectivity: A review. *Brain Connectivity*, *1*(1), 13–36. https://doi.org/10.1089/brain.2011.0008

Friston, K. J., Williams, S., Howard, R., Frackowiak, R. S., & Turner, R. (1996). Movement-related effects in fMRI time-series. *Magnetic Resonance in Medicine*, *35*(3), 346–355. https://doi.org/10.1002/mrm.1910350312

Gilman, S., Wenning, G. K., Low, P. A., Brooks, D. J., Mathias, C. J., Trojanowski, J. Q., Wood, N. W., Colosimo, C., Durr, A., Fowler, C. J., Kaufmann, H., Klockgether, T., Lees, A., Poewe, W., Quinn, N., Revesz, T., Robertson, D., Sandroni, P., Seppi, K., & Vidailhet, M. (2008). Second consensus statement on the diagnosis of multiple system atrophy. *Neurology*, *71*(9), 670–676. https://doi.org/10.1212/01.wnl.0000324625.00404.15

Godefroy, O. (2003). Frontal syndrome and disorders of executive functions. *Journal of Neurology*, *250*(1), 1–6. https://doi.org/10.1007/s00415-003-0918-2

Hänggi, J., Streffer, J., Jäncke, L., & Hock, C. (2011). Volumes of lateral temporal and parietal structures distinguish between healthy aging, mild cognitive impairment, and Alzheimer's disease. *Journal of Alzheimer's Disease*, *26*(4), 719–734. https://doi.org/10.3233/JAD-2011-101260

He, Y., Wang, L., Zang, Y., Tian, L., Zhang, X., Li, K., & Jiang, T. (2007). Regional coherence changes in the early stages of Alzheimer's disease: A combined structural and resting-state functional MRI study. *NeuroImage*, *35*, 488–500. https://doi.org/10.1016/j.neuroimage.2006.11.042

Henson, R. N., Burgess, N., & Frith, C. D. (2000). Recoding, storage, rehearsal and grouping in verbal short-term memory: An fMRI study. *Neuropsychologia*, *38*(4), 426–440. https://doi.org/10.1016/s0028-3932(99)00098-6

Homma, T., Mochizuki, Y., Komori, T., & Isozaki, E. (2016). Frequent globular neuronal cytoplasmic inclusions in the medial temporal region as a possible characteristic feature in multiple system atrophy with dementia. *Neuropathology*, *36*(5), 421–431. https://doi.org/10.1111/neup.12289

Hoops, S., Nazem, S., Siderowf, A. D., Duda, J. E., Xie, S. X., Stern, M. B., & Weintraub, D. (2009). Validity of the MoCA and MMSE in the detection of MCI and dementia in Parkinson disease. *Neurology*, *73*(21), 1738–1745. https://doi.org/10.1212/WNL.0b013e3181c34b47

Hu, H., Chen, J., Huang, H., Zhou, C., Zhang, S., Liu, X., Wang, L., Chen, P., Nie, K., Chen, L., Wang, S., Huang, B., & Huang, R. (2020). Common and specific altered amplitude of low-frequency fluctuations in Parkinson's disease patients with and without freezing of gait in different frequency bands. *Brain Imaging and Behavior*, *14*(3), 857–868. https://doi.org/10.1007/s11682-018-0031-x

Ibrahim, B., Suppiah, S., Ibrahim, N., Mohamad, M., Hassan, H., Nasser, N., & Saripan, M. I. (2021). Diagnostic power of resting-state fMRI for detection of network connectivity in Alzheimer's disease and mild cognitive impairment: A systematic review. *Human Brain Mapping*, *42*(9), 2941–2968. https://doi.org/10.1002/hbm.25369

Jellinger, K. A., Seppi, K., & Wenning, G. K. (2005). Grading of neuropathology in multiple system atrophy: Proposal for a novel scale. *Movement Disorders*, *20*(Suppl 12), S29–S36. https://doi.org/10.1002/mds.20537

Jones, D., Machulda, M., Vemuri, P., McDade, E., Zeng, G., Senjem, M., Gunter, J. L., Przybelski, S. A., Avula, R. T., Knopman, D. S., Boeve, B. F., Petersen, R. C., & Jack, C. R. (2011). Age-related changes in the default mode network are more advanced in Alzheimer disease. *Neurology*, *77*(16), 1524–1531. https://doi.org/10.1212/WNL.0b013e318233b33d

Jones, D. T., Knopman, D. S., Gunter, J. L., Graff-Radford, J., Vemuri, P., Boeve, B. F., Petersen, R. C., Weiner, M. W., Jack, C. R., Jr., & Alzheimer's Disease Neuroimaging Initiative. (2016). Cascading network failure across the Alzheimer's disease spectrum. *Brain*, *139*(Pt 2), 547–562. https://doi.org/10.1093/brain/awv338

Kawabata, K., Hara, K., Watanabe, H., Bagarinao, E., Ogura, A., Masuda, M., Yokoi, T., Kato, T., Ohdake, R., Ito, M., Katsuno, M., & Sobue, G. (2019). Alterations in cognition-related cerebello-cerebral networks in multiple system atrophy. *Cerebellum*, *18*(4), 770–780. https://doi.org/10.1007/s12311-019-01031-7

Kawai, Y., Suenaga, M., Takeda, A., Ito, M., Watanabe, H., Tanaka, F., Kato, K., Fukatsu, H., Naganawa, S., Kato, T., Ito, K., & Sobue, G. (2008). Cognitive impairments in multiple system atrophy: MSA-C vs MSA-P. *Neurology*, *70*(16 Pt 2), 1390–1396. https://doi.org/10.1212/01.wnl.0000310413.04462.6a

Kim, J. S., Yang, J. J., Lee, D. K., Lee, J. M., Youn, J., & Cho, J. W. (2015). Cognitive impairment and its structural correlates in the Parkinsonian subtype of multiple system atrophy. *Neuro-Degenerative Diseases*, *15*(5), 294–300. https://doi.org/10.1159/000430953

Koga, S., Aoki, N., Uitti, R. J., van Gerpen, J. A., Cheshire, W. P., Josephs, K. A., Wszolek, Z. K., Langston, J. W., & Dickson, D. W. (2015). When DLB, PD, and PSP masquerade as MSA: An autopsy study of 134 patients. *Neurology*, *85*(5), 404–412. https://doi.org/10.1212/WNL.0000000000001807

Koga, S., Parks, A., Uitti, R. J., van Gerpen, J. A., Cheshire, W. P., Wszolek, Z. K., & Dickson, D. W. (2017). Profile of cognitive impairment and underlying pathology in multiple system atrophy. *Movement Disorders*, *32*(3), 405–413. https://doi.org/10.1002/mds.26874

Lee, M. J., Shin, J. H., Seoung, J. K., Lee, J. H., Yoon, U., Oh, J. H., Jung, D. S., & Kim, E. J. (2016). Cognitive impairments associated with morphological changes in cortical and subcortical structures in multiple system atrophy of the cerebellar type. *European Journal of Neurology*, *23*(1), 92–100. https://doi.org/10.1111/ene.12796

Litvan, I., Goldman, J. G., Tröster, A. I., Schmand, B. A., Weintraub, D., Petersen, R. C., Mollenhauer, B., Adler, C. H., Marder, K., Williams-Gray, C. H., Aarsland, D., Kulisevsky, J., Rodriguez-Oroz, M. C., Burn, D. J., Barker, R. A., & Emre, M. (2012). Diagnostic criteria for mild cognitive impairment in Parkinson's disease: Movement Disorder Society Task Force guidelines. *Movement Disorders*, *27*(3), 349–356. https://doi.org/10.1002/mds.24893

Liu, X., Tu, Y., Zang, Y., Wu, A., Guo, Z., & He, J. (2019). Disrupted regional spontaneous neural activity in mild cognitive impairment patients with depressive symptoms: A resting-state fMRI study. *Neural Plasticity*, *2019*, 2981764. https://doi.org/10.1155/2019/2981764

Lyoo, C. H., Jeong, Y., Ryu, Y. H., Lee, S. Y., Song, T. J., Lee, J. H., Rinne, J. O., & Lee, M. S. (2008). Effects of disease duration on the clinical features and brain glucose metabolism in patients with mixed type multiple system atrophy. *Brain*, *131*(Pt 2), 438–446. https://doi.org/10.1093/brain/awm328

Mandal, P., Banerjee, A., Tripathi, M., & Sharma, A. (2018). A comprehensive review of magnetoencephalography (MEG) studies for brain functionality in healthy aging and Alzheimer's disease (AD). *Frontiers in Computational Neuroscience*, *12*, 60. https://doi.org/10.3389/fncom.2018.00060

Menon, V. (2011). Large-scale brain networks and psychopathology: A unifying triple network model. *Trends in Cognitive Sciences*, *15*(10), 483–506. https://doi.org/10.1016/j.tics.2011.08.003

Menon, V. (2015). Large-scale functional brain organization. *Brain Mapping*, *2*, 449–459.

Minnerop, M., Specht, K., Ruhlmann, J., Schimke, N., Abele, M., Weyer, A., Wüllner, U., & Klockgether, T. (2007). Voxel-based morphometry and voxel-based relaxometry in multiple system atrophy-a comparison between clinical subtypes and correlations with clinical parameters. *NeuroImage*, *36*(4), 1086–1095. https://doi.org/10.1016/j.neuroimage.2007.04.028

Ng, K. K., Lo, J. C., Lim, J., Chee, M., & Zhou, J. (2016). Reduced functional segregation between the default mode network and the executive control network in healthy older adults: A longitudinal study. *NeuroImage*, *133*, 321–330. https://doi.org/10.1016/j.neuroimage.2016.03.029

Putcha, D., Ross, R. S., Cronin-Golomb, A., Janes, A. C., & Stern, C. E. (2015). Altered intrinsic functional coupling between core neurocognitive networks in Parkinson's disease. *NeuroImage. Clinical*, *7*, 449–455. https://doi.org/10.1016/j.nicl.2015.01.012

Quinn, N. (1989). Multiple system atrophy – The nature of the beast. *Journal of Neurology, Neurosurgery, and Psychiatry*, *52*(Suppl), 78–89. https://doi.org/10.1136/jnnp.52.suppl.78

Quinn, N. (2020). Multiple system atrophy: The nature of the beast revisited. *Journal of Neurology, Neurosurgery, and Psychiatry*, *91*(1), 3–4. https://doi.org/10.1136/jnnp-2018-318187

Raichle, M. E. (2015). The brain's default mode network. *Annual Review of Neuroscience*, *38*, 433–447. https://doi.org/10.1146/annurev-neuro-071013-014030

Salvesen, L., Winge, K., Brudek, T., Agander, T. K., Løkkegaard, A., & Pakkenberg, B. (2017). Neocortical neuronal loss in patients with

multiple system atrophy: A stereological study. *Cerebral Cortex*, *27*(1), 400–410. https://doi.org/10.1093/cercor/bhv228

Sambati, L., Calandra-Buonaura, G., Giannini, G., Cani, I., Provini, F., Poda, R., Oppi, F., Stanzani Maserati, M., & Cortelli, P. (2020). Cognitive profile and its evolution in a cohort of multiple system atrophy patients. *Frontiers in Neurology*, *11*, 537360. https://doi.org/10.3389/fneur.2020.537360

Schmahmann, J. D., Guell, X., Stoodley, C. J., & Halko, M. A. (2019). The theory and neuroscience of cerebellar cognition. *Annual Review of Neuroscience*, *42*, 337–364. https://doi.org/10.1146/annurev-neuro-070918-050258

Schmahmann, J. D., & Sherman, J. C. (1998). The cerebellar cognitive affective syndrome. *Brain*, *121*(Pt 4), 561–579. https://doi.org/10.1093/brain/121.4.561

Seeley, W. W., Menon, V., Schatzberg, A. F., Keller, J., Glover, G. H., Kenna, H., Reiss, A. L., & Greicius, M. D. (2007). Dissociable intrinsic connectivity networks for salience processing and executive control. *The Journal of Neuroscience*, *27*(9), 2349–2356. https://doi.org/10.1523/JNEUROSCI.5587-06.2007

Shen, C., Chen, Q. S., Zuo, C. T., Liu, F. T., & Wang, J. (2022). The frontal and cerebellar metabolism related to cognitive dysfunction in multiple system atrophy. *Frontiers in Aging Neuroscience*, *14*, 788166. https://doi.org/10.3389/fnagi.2022.788166

Shin, N. Y., Bang, M., Yoo, S. W., Kim, J. S., Yun, E., Yoon, U., Han, K., Ahn, K. J., & Lee, S. K. (2021). Cortical thickness from MRI to predict conversion from mild cognitive impairment to dementia in Parkinson disease: A machine learning-based model. *Radiology*, *300*(2), 390–399. https://doi.org/10.1148/radiol.2021203383

Skidmore, F. M., Yang, M., Baxter, L., von Deneen, K. M., Collingwood, J., He, G., White, K., Korenkevych, D., Savenkov, A., Heilman, K. M., Gold, M., & Liu, Y. (2013). Reliability analysis of the resting state can sensitively and specifically identify the presence of Parkinson disease. *NeuroImage*, *75*, 249–261. https://doi.org/10.1016/j.neuroimage.2011.06.056

Stankovic, I., Krismer, F., Jesic, A., Antonini, A., Benke, T., Brown, R. G., Burn, D. J., Holton, J. L., Kaufmann, H., Kostic, V. S., Ling, H., Meissner, W. G., Poewe, W., Semnic, M., Seppi, K., Takeda, A., Weintraub, D., Wenning, G. K., & Movement Disorders Society MSA (MODIMSA) Study Group. (2014). Cognitive impairment in multiple system atrophy: A position statement by the Neuropsychology Task Force of the MDS Multiple System Atrophy (MODIMSA) study group. *Movement Disorders*, *29*(7), 857–867. https://doi.org/10.1002/mds.25880

Strick, P. L., Dum, R. P., & Fiez, J. A. (2009). Cerebellum and nonmotor function. *Annual Review of Neuroscience*, *32*, 413–434. https://doi.org/10.1146/annurev.neuro.31.060407.125606

Tang, S., Wang, Y., Liu, Y., Chau, S. W., Chan, J. W., Chu, W. C., Abrigo, J. M., Mok, V. C. T., & Wing, Y. K. (2022). Large-scale network dysfunction in α-synucleinopathy: A meta-analysis of resting-state functional connectivity. *EBioMedicine*, *77*, 103915. https://doi.org/10.1016/j.ebiom.2022.103915

Todd, J. J., & Marois, R. (2004). Capacity limit of visual short-term memory in human posterior parietal cortex. *Nature*, *428*(6984), 751–754. https://doi.org/10.1038/nature02466

Uddin, L. Q., Supekar, K., Amin, H., Rykhlevskaia, E., Nguyen, D. A., Greicius, M. D., & Menon, V. (2010). Dissociable connectivity within human angular gyrus and intraparietal sulcus: Evidence from functional and structural connectivity. *Cerebral Cortex*, *20*(11), 2636–2646. https://doi.org/10.1093/cercor/bhq011

Wang, N., Edmiston, E. K., Luo, X., Yang, H., Chang, M., Wang, F., & Fan, G. (2017). Comparing abnormalities of amplitude of low-frequency fluctuations in multiple system atrophy and idiopathic Parkinson's disease measured with resting-state fMRI. *Psychiatry Research. Neuroimaging*, *269*, 73–81. https://doi.org/10.1016/j.pscychresns.2017.09.002

Wang, Z., Liu, Y., Ruan, X., Li, Y., Li, E., Zhang, G., Li, M., & Wei, X. (2020). Aberrant amplitude of low-frequency fluctuations in different frequency bands in patients with Parkinson's disease. *Frontiers in Aging Neuroscience*, *12*, 576682. https://doi.org/10.3389/fnagi.2020.576682

Wenning, G. K., Tison, F., Ben Shlomo, Y., Daniel, S. E., & Quinn, N. P. (1997). Multiple system atrophy: A review of 203 pathologically proven cases. *Movement Disorders*, *12*(2), 133–147. https://doi.org/10.1002/mds.870120203

Yan, R., Huang, Y., Shi, J., Zou, H., Wang, X., Xia, Y., Zhao, S., Zhou, H. L., Chen, Y., Li, X. S., Wu, X. X., Yao, Z. J., & Lu, Q. (2022). Alterations of regional spontaneous neuronal activity and corresponding brain circuits related to non-suicidal self-injury in young adults with major depressive disorder. *Journal of Affective Disorders*, *305*, 8–18. https://doi.org/10.1016/j.jad.2022.02.040

Yang, H., Luo, X., Yu, H., Guo, M., Cao, C., Li, Y., & Fan, G. (2020). Altered resting-state voxel-level whole-brain functional connectivity in multiple system atrophy patients with cognitive impairment. *Clinical Neurophysiology*, *131*(1), 54–62. https://doi.org/10.1016/j.clinph.2019.09.026

Yang, H., Wang, N., Luo, X., Lv, H., Liu, H., & Fan, G. (2019a). Altered functional connectivity of dentate nucleus in parkinsonian and cerebellar variants of multiple system atrophy. *Brain Imaging and Behavior*, *13*(6), 1733–1745. https://doi.org/10.1007/s11682-019-00097-5

Yang, H., Wang, N., Luo, X., Lv, H., Liu, H., Li, Y., & Fan, G. (2019b). Cerebellar atrophy and its contribution to motor and cognitive performance in multiple system atrophy. *NeuroImage. Clinical*, *23*, 101891. https://doi.org/10.1016/j.nicl.2019.101891

Yang, L., Yan, Y., Wang, Y., Hu, X., Lu, J., Chan, P., Yan, T., & Han, Y. (2018). Gradual disturbances of the amplitude of Low-frequency fluctuations (ALFF) and fractional ALFF in Alzheimer spectrum. *Frontiers in Neuroscience*, *12*, 975–990. https://doi.org/10.3389/fnins.2018.00975

Zang, Y. F., He, Y., Zhu, C. Z., Cao, Q. J., Sui, M. Q., Liang, M., Tian, L. X., Jiang, T. Z., & Wang, Y. F. (2007). Altered baseline brain activity in children with ADHD revealed by resting-state functional MRI. *Brain & Development*, *29*(2), 83–91. https://doi.org/10.1016/j.braindev.2006.07.002

Zhang, L., Cao, B., Zou, Y., Wei, Q. Q., Ou, R., Zhao, B., Yang, J., Wu, Y., & Shang, H. (2019). Frontal lobe function, behavioral changes and quality of life in patients with multiple system atrophy. *Restorative Neurology and Neuroscience*, *37*(1), 11–19. https://doi.org/10.3233/RNN-180862

Zuo, X. N., & Xing, X. X. (2014). Test-retest reliabilities of resting-state FMRI measurements in human brain functional connectomics: A systems neuroscience perspective. *Neuroscience and Biobehavioral Reviews*, *45*, 100–118. https://doi.org/10.1016/j.neubiorev.2014.05.009

SUPPORTING INFORMATION

Additional supporting information can be found online in the Supporting Information section at the end of this article.

How to cite this article: Li, Y., Liu, H., Yu, H., Yang, H., Guo, M., Cao, C., Pang, H., Liu, Y., Cao, K., & Fan, G. (2023). Alterations of voxel-wise spontaneous activity and corresponding brain functional networks in multiple system atrophy patients with mild cognitive impairment. *Human Brain Mapping*, *44*(2), 403–417. https://doi.org/10.1002/hbm.26058